

# The Connection between Discrete- and Continuous-Time Descriptions of Gaussian Continuous Processes

Federica Ferretti,<sup>1,2</sup> Victor Chardès,<sup>3</sup> Thierry Mora,<sup>3</sup> Aleksandra M Walczak,<sup>3</sup> and Irene Giardina<sup>1,2,4</sup>

<sup>1</sup>*Dipartimento di Fisica, Università Sapienza, 00185 Rome, Italy*

<sup>2</sup>*Istituto Sistemi Complessi, Consiglio Nazionale delle Ricerche, UOS Sapienza, 00185 Rome, Italy*

<sup>3</sup>*Laboratoire de Physique de l'École Normale supérieure (PSL University),*

*CNRS, Sorbonne Université, Université de Paris, 75005 Paris, France*

<sup>4</sup>*INFN, Unità di Roma 1, 00185 Rome, Italy*

(Dated: November 1, 2021)

Learning the continuous equations of motion from discrete observations is a common task in all areas of physics. However, not any discretization of a Gaussian continuous-time stochastic process can be adopted in parametric inference. We show that discretizations yielding consistent estimators have the property of ‘invariance under coarse-graining’, and correspond to fixed points of a renormalization group map on the space of autoregressive moving average (ARMA) models (for linear processes). This result explains why combining differencing schemes for derivatives reconstruction and local-in-time inference approaches does not work for time series analysis of second or higher order stochastic differential equations, even if the corresponding integration schemes may be acceptably good for numerical simulations.

*Introduction* — How to properly connect discrete-time descriptions of stochastic processes to their continuous-time counterparts is a key problem in time series analysis and dynamical modelling. It is a common situation to observe the evolution of a system through discrete sequences of experimental data, and try to learn a continuous model from these observations. A principled way to proceed is to introduce physically motivated assumptions in the form of stochastic differential equations (SDEs), and adopt Bayesian or non-Bayesian parametric approaches to infer a parameter-free model. Independently of the chosen approach, adopting a consistent discretization is crucial to link experimental data with theory.

In particular, the issue cannot be overlooked when there is no direct experimental access to the full dynamical state of the system, i.e. a point in phase space where trajectories are Markovian. Partial observation of the degrees of freedom of a system leads to the loss of Markovianity, a fact which poses big challenges to dynamical inference tasks. These issues are typically addressed using numerical marginalization methods for Hidden Markov Models, which are laborious to implement in many realistic instances [1]. It may then be tempting to attempt state space reconstruction through delay vectors or equivalent tools [2].

However, the stochastic nature of the system sets strong limits to state space reconstruction: contrarily to the deterministic case [3], there is no theorem that guarantees the existence of a finite-dimensional embedding restoring the Markov nature of the dynamics, when the observed process is directly or indirectly driven by dynamical noise. An example of physical relevance is that of underdamped Langevin processes, described by second order SDEs, where measurement consists of an arbitrarily accurate projection onto the inertial coordinate. In

this work we will mainly focus on this class of processes, even if the meaning of our results is general.

The second context where discretization is essential is that of numerical simulations. Several methods for the integration of SDEs have been proposed and extensively studied, with special attention to convergence and stability analysis [4]. The simplest among them is the Euler-Maruyama scheme, which corresponds, in time series analysis, to the introduction of a delay vector to reconstruct the derivatives. It is known that this integration scheme is convergent in the limit of vanishing increments. Interestingly, however, the same scheme fails when used to infer the continuous model from the data, even asymptotically. A different behavior might therefore occur when a given discretization is used for inference or numerical integration purposes.

In this Letter we try to formalize this difference at its core. Our aim is to understand why certain schemes seem to work for integration and not for inference and, more broadly, what are the general properties of a good discretization procedure. Restricting to linear processes, we identify discretizations yielding consistent estimators, when adopted in parametric inference approaches, with the fixed points of a Renormalization Group (RG) map on the space of discrete-time autoregressive moving average (ARMA) models. In this way, we provide an argument for the inadequacy of all purely autoregressive models of order  $p > 1$  ( $AR(p)$ ) – corresponding to naive exploitation of delay vectors – as discretizations of generalized continuous-time Langevin equations. We then suggest a possible *effective* Euler-like discretization of underdamped Langevin equations, which can be derived as a consequence of the fluctuation-dissipation relation and is only valid for equilibrium processes.

*AR(2) models* — Given an ideally infinite sequence  $\{X_n\}_{n \in \mathbb{N}}$  of measured points, in one or higher dimension,

suppose it is generated by a stochastic process of the form

$$dx = v dt; \quad dv = a(x, v)dt + b(x, v)dW, \quad (1)$$

where  $W(t)$  is a Wiener process and  $a, b$  are arbitrary functions. The simplest thing to do in order to reconstruct from those measurements the underlying Markov dynamics is to estimate the velocities through finite differences. Let the reconstructed velocities be  $\bar{V}_n = (X_{n+1} - X_n)/\tau$ , assuming a homogeneous step  $\tau$  along the whole trajectory. Replacing the time series  $\{X_n\}_{n \in \mathbb{N}}$  with  $\{(X_n, \bar{V}_n)\}_{n \in \mathbb{N}}$  does not provide an embedding with proper Markov properties, in general. This approach corresponds indeed to adopting a Euler discretization.

The failure of Euler and Milstein schemes in time-series analysis of second order processes has been observed from both a Bayesian [5–7] and a non-Bayesian perspective [8–11]. Problems arise from the fact that the associated Taylor-Itô expansion is truncated too early to approximate correctly the noisy term, and manifest themselves through the inconsistency of parameter estimators, even in the  $\tau \rightarrow 0$  limit. The required minimum order of convergence to find consistent estimators is  $3/2$ , corresponding to SDE integration algorithms like [12–14].

The consequences of this incorrect approximation are also visible when the Euler scheme is used to simulate the continuous process, even though the integration algorithm is convergent. To elucidate this fact, we employ the Euler algorithm to simulate a linear equilibrium process of the kind in Eq. (1) with  $a(x, v) = -\eta v - kx$  and  $b(x, v) = \sqrt{2T\eta}$ . An analytical solution for the stationary self-correlation  $C(t) = \langle x(t_0)x(t_0 + t) \rangle$  can be computed in this case:

$$C(t) = e^{-\gamma t} \frac{T}{k} \left[ \cos(\sqrt{k - \gamma^2}t) + \gamma \frac{\sin(\sqrt{k - \gamma^2}t)}{\sqrt{k - \gamma^2}} \right], \quad (2)$$

with  $\gamma = \eta/2$ .

Eq. (2) gives the values of the first three derivatives at  $t = 0$ :  $C(0) = T/k$ ,  $\dot{C}(0) = 0$ ,  $\ddot{C}(0) = -T$ ,  $\ddot{C}(0) = 2\gamma T$ . In principle it is sufficient to reconstruct only a triplet of close points,  $C(0), C(\tau), C(2\tau)$ , and extract from proper combinations all the parameters of the continuous model:  $T, \eta, k$ . The empirical correlation function from the simulated trajectory looks identical to Eq. (2) on typical observation scales ( $\tau > 1$  in Fig. 1a), but fluctuations of the order of  $\tau^3$  are not correctly reproduced on scales  $\tau \sim \tau_{sim}$ . This fact is made visible by the estimation of  $\eta$  from the first triplet of points of the empirical correlation function shown in Fig. 1c.

We perform simulations of the process with  $\eta^{true} = 1$  and fixed integration steps,  $\tau_{sim}$ . We then filter the simulated trajectory by selecting observation time steps  $\tau = n\tau_{sim}$ , with varying  $n$ . When  $\tau = \tau_{sim}$  the inferred value of  $\eta$  is  $3/2\eta^{true}$  – cf. Ref. [7]. Since we used the exact solution Eq. (2) to extract  $\eta$ , this discrepancy indicates that numerical data do not reproduce correctly the

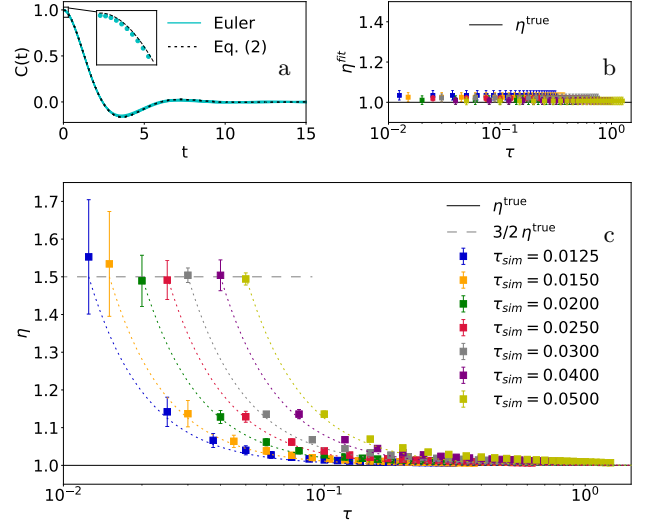


FIG. 1: (a) Empirical curves for  $C(t)$ , obtained from simulations at different  $\tau_{sim}$ . The black dotted line corresponds to the exact analytical prediction from Eq. (2). (b) No bias affects  $\eta^{fit}$ , which we estimate from a fit of Eq. (2) on the curves in Fig. a. (c) Estimates of  $\eta$  from Euler-generated time series. All simulations are performed with the same parameter values:  $\eta = T = k = 1$ . Time steps between subsequently observed points are integer multiples of  $\tau_{sim}$ . For any  $\tau$ , we use the same inference formulas involving the first 3 observed points of  $C(t)$  to extract the parameters (additional information in SM [15]). When  $\tau = \tau_{sim}$   $\eta$  is biased of a factor  $3/2$ , which is progressively reduced as  $\tau$  is increased. The decay of the bias is predicted from Eq. (9) as  $3/(2\alpha_3^l)$ , identifying  $n = \tau/\tau_{sim} = 2^l$  (dotted lines).

properties of the continuous process on scale  $\tau_{sim}$  [20]. As we coarse-grain the simulated time series, the estimation bias on the damping parameter is progressively reduced. Alternatively, fitting the correlation curve with Eq. (2) over large time intervals gives unbiased estimates, as shown in Fig. 1b.

We conclude that while the Euler discretization is not consistent with continuous underdamped Langevin models at short scales, it appropriately describes the dynamics on the larger scales. Hence it can be successfully employed in approximate numerical simulations, as it is possible to choose a small integration step compared to the observation scale of the process. This separation of scales cannot occur in the case of state space inference, where we look at the system's evolution exactly at the scale of the discretization.

*RG for ARMA models* — Viewing the approach to continuum as a progressive increase in the number of iterations within a given time window inspires a way to characterize a *good* discretization scheme through the property of invariance under coarse graining. In other words, we require that, when  $\tau$  is small enough, integrating the process through a single step on a time interval  $\tau$

or through a combination of two integration steps on intervals of amplitude  $\tau/2$  should provide the same result. Notice that this property is not equivalent to nor implied by the convergence of the integration scheme.

Within this framework, the problem of connecting discrete models with continuous ones can be addressed for general processes. The natural tool to use is the Renormalization Group (RG). We focus on the linear case, for which the RG procedure can be carried out explicitly and without approximations. We combine a Migdal-Kadanoff decimation procedure [16] on the discrete model of interest with an asymptotic series expansion in  $\tau$  for the parameters of the process. Since our motivation comes from the study of inertial processes, the discussion refers to autoregressive moving-average (ARMA) models of order  $p = 2$  (some generalization can be found in the Supplemental Material [15]). An ARMA( $p, q$ ) process is defined by the following update equation [17]:

$$X_n = \sum_{i=1}^p \phi_i X_{n-i} + \sum_{i=1}^q \nu_i \epsilon_{n-i} + \mu \epsilon_n, \quad (3)$$

with  $\phi_i, \nu_i, \mu \in \mathbb{R}$ , and  $\epsilon_m \sim \mathcal{N}(0, 1)$  I.I.D. The autoregressive (AR) part consists of a contribution from the  $p$  past states of the dynamical variable, while the moving average (MA) part refers to the contribution of the stochastic noise up to  $q$  steps in the past.

Let us start by considering the process in Eq. (1), with  $a(x, v) = -\eta v - kx$  and  $b(x, v) = b$ . When discretized using the Euler scheme and projected onto the  $x$  subspace, the dynamical equations take the form of an AR(2) model

$$X_n = \sum_{i=1}^2 \phi_i X_{n-i} + \sigma \epsilon_n, \quad (4)$$

with  $\phi_1 = 2 - \eta\tau$ ,  $\phi_2 = -(1 - \eta\tau + k\tau^2)$ ,  $\sigma^2 = b^2\tau^3$ . Decimation of the time series generated by Eq. (4) yields, from the first iteration, a linear model of the form of Eq. (3) with  $p = 2$  and  $q = 1$  – ARMA(2,1). The ARMA(2,1) structure remains unchanged during the next iterations of the RG map, so we detail the RG procedure for this class of models. It is built upon the analogy between the time series and a one-dimensional spin chain: at each iteration, the goal is to get rid of the ‘sub-lattice of odd sites’, and then rescale the obtained coarse-grained dynamics in order to bring it back to a time step of amplitude  $\tau$ .

At the  $l$ -th iteration, we start from the difference equation:

$$X_n = \sum_{i=1}^2 \phi_i^l X_{n-i} + r_n^l \quad \text{with} \quad r_n^l = \mu^l \epsilon_n + \nu^l \epsilon_{n-1}. \quad (5)$$

Decimation of the series is performed by combining neighboring equations in the following way:  $X_n + \phi_1^l X_{n-1} - \phi_2^l X_{n-2}$  (see SM [15]). This combination yields

an effective difference equation describing the evolution of states at even temporal sites: it is again an ARMA(2,1) process with autoregressive coefficients  $\tilde{\phi}_1^l, \tilde{\phi}_2^l$  and moving average coefficients  $\tilde{\mu}^l, \tilde{\nu}^l$ . After rescaling the time step,  $2\tau \rightarrow \tau$ , parameters are correspondingly rescaled as  $\tilde{\phi}_i^l \rightarrow \phi_i^{l+1}$ ,  $\tilde{\mu}^l \rightarrow \mu^{l+1}$  and  $\tilde{\nu}^l \rightarrow \nu^{l+1}$ . Notice that these parameters are dimensionless and  $\tau$  does not appear explicitly in Eq. (5). Their dependency on  $\tau$  is however what determines whether the ARMA process is a discretization of a continuous-time model or not.

We express then  $\phi_{1,2}$  and  $\mu, \nu$  as asymptotic power series of  $\tau$  and work, up to the desired order, with recursive relations for the coefficients of the series expansion. The physical dimension of each coefficient is now set by the order of the corresponding term, and they are rescaled, after coarse graining, according to it. The assumption of asymptoticity of the series enables to truncate it to a finite order and reduce the analysis to a finite-dimensional space of parameters, whereas fixed points are in principle specified by four functions:  $\phi_{1,2}^*(\tau), \mu^*(\tau), \nu^*(\tau)$ .

Since the flow of the autoregressive coefficients does not depend on moving average terms, a layered set of recurrence relations is found (SM [15]). To work out the stochastic part of the equation, it is convenient to introduce running parameters  $\alpha$  and  $\beta$ , defined as:

$$\alpha = \mathbb{E}[r_n^2] = \mu^2 + \nu^2; \quad \beta = \mathbb{E}[r_n r_{n\pm 1}] = \mu\nu. \quad (6)$$

Starting from Eq. (4) (Euler discretization) implies  $\beta = 0$ . Since the first iteration, however, RG transforms AR(2) models into ARMA(2,1). Random increments are expressed hereafter as combinations of lagged I.I.D. variables, resulting in correlations across neighboring time steps ( $\beta \neq 0$ ), which represent the discrete counterpart of color [18, 19]. Color is the key missing ingredient in the Euler scheme, from which the bias discussed above originates.

Our goal is to find the fixed points of the RG map. We solve the recurrence relations for the coefficients of the series expansions of AR and MA coefficients:

$$\phi_1 = \sum_{k=0}^{\infty} \psi_k \tau^k, \quad \phi_2 = \sum_{k=0}^{\infty} \theta_k \tau^k; \quad (7)$$

$$\alpha = \sum_{k=0}^{\infty} \alpha_k \tau^k, \quad \beta = \sum_{k=0}^{\infty} \beta_k \tau^k. \quad (8)$$

There are four manifolds of fixed points in the space of linear ARMA(2,1) models. Their description up to the third order in  $\tau$  is provided in Table I.

The projection of the fixed point manifolds on the plane of leading order AR coefficients,  $\phi_0$  and  $\theta_0$ , is shown in Fig. 2. The asymptotically stable fixed point A in Fig. 2 is a model with both moving average and autoregressive order equal to zero, i.e. a sequence of independent random variables. Fixed point B is an AR(1)

TABLE I: Fixed point solutions of RG recurrence relations up to third order in  $\tau$ . We find 4 types of processes, parametrized by the arbitrary constants  $u$ ,  $s$ ,  $z$  and  $b$ . In addition to the reported ones, there are diverging fixed points.

Model	AR coefficients								MA coefficients							
	$\psi_0^*$	$\theta_0^*$	$\psi_1^*$	$\theta_1^*$	$\psi_2^*$	$\theta_2^*$	$\psi_3^*$	$\theta_3^*$	$\alpha_0^*$	$\beta_0^*$	$\alpha_1^*$	$\beta_1^*$	$\alpha_2^*$	$\beta_2^*$	$\alpha_3^*$	$\beta_3^*$
A. MA(0)	0	0	0	0	0	0	0	0	$s$	0	0	0	0	0	0	0
B. AR(1)	1	0	$u$	0	$u^2/2$	0	$u^3/6$	0	0	0	$s$	0	$us$	0	$2u^2s/3$	0
C. ARMA(2,1)	-1	-1	$u$	$2u$	$-u^2/2$	$-2u^2$	$u^3/6$	$(2u)^3/6$	0	0	$4s$	$s$	$-8us$	$-2us$	$32u^2s/3$	$13u^2s/6$
D. ARMA(2,1)	2	-1	$u$	$-u$	$z$	$-u^2/2$	$u(6z - u^2)/12$	$-u^3/6$	0	0	$-2s$	$s$	$-2us$	$us$	$4b - (2z + 3u^2)s$	$b$

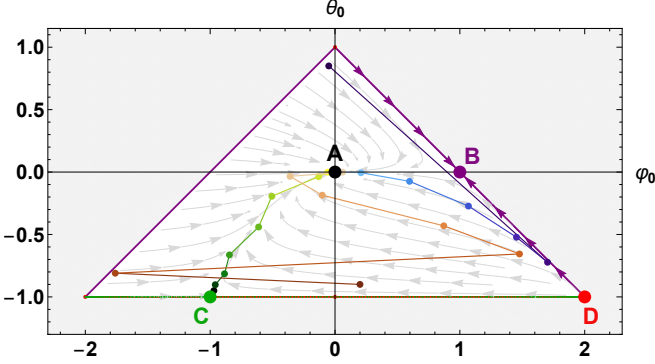


FIG. 2: Fixed points of the RG map on the plane of leading order AR coefficients,  $\psi_0$ ,  $\theta_0$ . The interior of the triangle is the basin of attraction (b.o.a.) of the stable fixed point A. The purple sides are the b.o.a. of the AR(1) fixed point B. The b.o.a.'s of fixed points C and D are contained in the basis of the triangle. The Euler AR(2) process we focused on has coordinates (2,-1) in this plane. Colored sequences of dots represent the solution of the recurrence relation from three sample initial conditions. Arrows show the direction of (discrete) moves and should not be interpreted as continuous flow lines.

process: it can be interpreted as a consistent discretization of a fully observed Markov process, described by a linear 1st-order SDE in continuous time. In addition to those, we have two other fixed point manifolds corresponding to proper ARMA(2,1) models. One of them (C in Fig. 2) is not a continuous process, but evolves through finite jumps; its properties are related to the details of the decimation. The other one (D) represents the consistent discretization of a partially observed two-dimensional Markov process. The coefficients  $\phi_1$  and  $\phi_2$  reconstruct at leading order a second derivative and, at first order, a linear damping term  $u\dot{x}$  appears on the r.h.s. of the SDE. Elastic forces are parametrized by  $z$  in Table I: if  $z = u^2/2$  such forces are absent and the model takes the structure of an integrated time series. The free parameter  $s$  reflects the  $O(\tau^{1/2})$  random contribution that is present when an independent Wiener process is added to the equation for the  $x$  variable in Eq. (1). Further details about this fixed point are in SM [15]. The following discussion mainly refers to purely in-

ertial models, described by linear underdamped Langevin equations. They can be seen as singular cases in the class of processes of fixed point D, constraining  $s = 0$ .

The AR(2) model in Eq. (4), which was obtained applying the Euler scheme to a linear underdamped process, falls in the basin of attraction of point D. The AR(2) model shares the same AR coefficients as the fixed point up to  $O(\tau^2)$ : what distinguishes it from a proper ARMA(2,1) process is the stochastic contribution. The initial conditions associated to the Euler AR(2) model Eq. (4) yield nontrivial recurrence relations for  $\alpha$  and  $\beta$  only from third order in the series expansion. Given  $(\alpha_3^0, \beta_3^0) = (1, 0)$ , associated to Eq. (4) with  $\sigma^2 = 1$ , the solution reads:

$$\alpha_3^l = \frac{2}{3} + \frac{1}{3}4^{-l}; \quad \beta_3^l = \frac{1}{6} - \frac{1}{6}4^{-l}. \quad (9)$$

At any lower order,  $k \leq 2$ , the coefficients  $\alpha_k$  and  $\beta_k$  are equal to zero. Eq. (9) shows an exponentially fast decay of  $\alpha_3$  and  $\beta_3$  to their asymptotic values, as also visible in Fig. 1. This fact means that after coarse graining of a few integration steps, the whole process is quite well reproduced even using the Euler scheme, whose order of strong convergence is  $1/2$ .

In the  $l \rightarrow \infty$  limit,  $\alpha_3^l \rightarrow 2/3$  and  $\beta_3^l \rightarrow 1/6$  and the resulting covariance matrix of the random increments takes the same form it would have if a discretization scheme convergent as  $\tau^{3/2}$  were applied. Taking  $l \rightarrow \infty$  is a way to achieve an effective  $\tau_{sim} \rightarrow 0$  limit for the original Euler discretization. Our analysis shows that this is the limit where the scheme works, and colored fluctuations are consistently reproduced through the acquired moving average (MA) structure.

Nonetheless, numerical and analytical findings in [7–10] hint at a possible *effective* discretization of generalized Langevin equations through AR(2) models. We remark that such models are inadequate: when applied to parametric inference problems, they produce biased estimators. However, on simple processes the bias manifests itself in a rather regular way. Precisely, for underdamped Langevin equations of the form:

$$dx = vdt; \quad dv = [-\eta vdt + f(x)]dt + \sqrt{2T\eta}dW, \quad (10)$$

it is fully absorbed by a  $\tau$ -independent rescaling factor

equal to  $2/3$  for the linear damping coefficient  $\eta$ , whereas the remaining parameters are unbiasedly estimated [7].

It is then natural to suggest the use of effective AR(2) time series corresponding to Euler discretizations with a rescaled damping coefficient  $\eta' = (2/3)\eta$ . In the simple case of the integrated Ornstein-Uhlenbeck process ( $f(x) = 0$ ), the result follows by just imposing thermal equilibrium at temperature  $T$  and consistency requirements. Although the derivation (SM [15]) is based on the linear and integrated nature of the process, we conjecture that the same fact should hold for all equilibrium inertial processes described by Eq. (S58), even in  $d > 1$  with  $f(x)$  a conservative force.

This effective white model reproduces – by construction – the features of the continuous-time model at the scale of  $\tau$  and guarantees the consistency of estimators when applied to dynamical inference problems. Of course, it cannot be used for simulations: taking an infinite number of iterations would converge to a continuous-time process with the wrong parameters. Only on the scale of  $\tau$  and – we conjecture – in the case of processes satisfying fluctuation dissipation relations, a working effective description can be obtained by rescaling the linear damping coefficient by  $2/3$  and neglecting color.

*Conclusion* — We defined an RG map on the space of all possible ARMA(2,1) processes, whose fixed points mark models obtained from consistent discretizations of stochastic processes in continuous time. The notion of consistency we use is related to the performance of the discretization scheme in parametric inference problems, and is different from that of convergence. The issue specifically regards the Euler-Maruyama scheme, which is important in this discussion due to its connection to the embedding problem.

Our RG analysis shows that, for partially observed processes, no finite number of delay vectors is capable of restoring the Markov nature of the dynamics. Any well-defined inference procedure should take this fact into account and always include color along with memory. The prescription is to add, for any delay vector, a corresponding delay in the noise term, thus transforming AR processes into ARMA processes. AR( $p$ ) processes with  $p > 1$  are indeed unstable under coarse graining: the attractor for all of them is a class of ARMA( $p, q$ ) processes with  $q = p - 1$ .

At the same time, the RG argument explains the success of the Euler scheme in simulations of underdamped linear processes. Beyond the limitations imposed by its order of convergence, the iterated integrator reproduces correctly even  $O(\tau^{3/2})$  fluctuations, in the  $(\tau/\tau_{sim}) \rightarrow \infty$  limit, if  $\tau$  is kept small. This separation of scales explains why, despite the inadequacy of the Euler scheme – and indeed of any AR(2) model – to discretize generalized Langevin equations, it practically works as an integrator but it is inappropriate when used to infer continuous equations from discretely sampled trajectories.

How to extend these results to nonlinear processes remains an open question.

The authors thank A. Cavagna, A. Vulpiani and A.C. Costa for helpful discussions. This work was partially supported by the ERC Consolidator Grant n. 724208, and by the Italian Ministry of Foreign Affairs and International Cooperation through the Adinmat project.

- 
- [1] S. Särkkä, *Bayesian Filtering and Smoothing* (Cambridge University Press, USA, 2013), ISBN 1107619289.
  - [2] M. Casdagli, S. Eubank, J. Farmer, and J. Gibson, *Physica D: Nonlinear Phenomena* **51**, 52 (1991), ISSN 0167-2789, URL <http://www.sciencedirect.com/science/article/pii/016727899190222U>.
  - [3] F. Takens, *Detecting strange attractors in turbulence* (Springer-Verlag, 1981), vol. 898, pp. 366–381.
  - [4] P. E. K. E. Platen and P. E. Kloeden, *Numerical Solution of Stochastic Differential Equations*, vol. 23 of *Stochastic Modelling and Applied Probability* (Springer-Verlag Berlin Heidelberg, 1992), 1st ed.
  - [5] A. Gloter, *Scandinavian Journal of Statistics* **33**, 83 (2006), <https://onlinelibrary.wiley.com/doi/pdf/10.1111/j.1467-9469.2006.00465.x>, URL <https://onlinelibrary.wiley.com/doi/abs/10.1111/j.1467-9469.2006.00465.x>.
  - [6] A. Gloter, *Statistics* **35**, 225 (2001), <https://doi.org/10.1080/02331880108802733>, URL <https://doi.org/10.1080/02331880108802733>.
  - [7] F. Ferretti, V. Chardès, T. Mora, A. M. Walczak, and I. Giardina, *Phys. Rev. X* **10**, 031018 (2020), URL <https://link.aps.org/doi/10.1103/PhysRevX.10.031018>.
  - [8] J. N. Pedersen, L. Li, C. Grădinaru, R. H. Austin, E. C. Cox, and H. Flyvbjerg, *Phys. Rev. E* **94**, 062401 (2016), URL <https://link.aps.org/doi/10.1103/PhysRevE.94.062401>.
  - [9] B. Lehle and J. Peinke, *Phys. Rev. E* **97**, 012113 (2018), URL <https://link.aps.org/doi/10.1103/PhysRevE.97.012113>.
  - [10] B. Lehle and J. Peinke, *Phys. Rev. E* **91**, 062113 (2015), URL <https://link.aps.org/doi/10.1103/PhysRevE.91.062113>.
  - [11] D. B. Brückner, P. Ronceray, and C. P. Broedersz, *Infering the non-linear dynamics of stochastic inertial systems* (2020), 2002.06680.
  - [12] R. D. Skeel and J. A. Izaguirre, *Molecular Physics* **100**, 3885 (2002), <https://doi.org/10.1080/0026897021000018321>, URL <https://doi.org/10.1080/0026897021000018321>.
  - [13] E. Vanden-Eijnden and G. Ciccotti, *Chemical Physics Letters* **429**, 310 (2006), ISSN 0009-2614, URL <http://www.sciencedirect.com/science/article/pii/S0009261406011092>.
  - [14] R. Mannella and V. Palleschi, *Phys. Rev. A* **40**, 3381 (1989), URL <https://link.aps.org/doi/10.1103/PhysRevA.40.3381>.
  - [15] See Supplemental Material at [URL will be inserted by publisher].

- [16] L. P. Kadanoff, *Annals of Physics* **100**, 359 (1976).
- [17] P. Brockwell and R. Davis, *Introduction to Time Series and Forecasting* (Springer, Berlin, 2002).
- [18] I. Horenko, C. Hartmann, C. Schütte, and F. Noe, *Phys. Rev. E* **76**, 016706 (2007), URL <https://link.aps.org/doi/10.1103/PhysRevE.76.016706>.
- [19] R. Zwanzig, *Nonequilibrium statistical mechanics* (Oxford University Press, USA, 2001).
- [20] We are here applying a correct formula (for the continuous process) to time series simulated via the Euler algorithm. In inference problems, the scenario is the opposite: the discretization scheme is employed to find inference formulas that are applied to sample trajectories of the continuous process. When inference formulas are local in time, the inaccuracies of the discretization emerge, be it in the data or in the equations.

**SUPPLEMENTAL MATERIAL:**

**The Connection Between Discrete- and Continuous-Time Descriptions of Gaussian Continuous Processes**

**I. ANALYSIS OF THE SIMULATED PROCESS**

In this section we provide a more detailed explanation of the procedure through which we obtained the results shown in Fig.1 in the main text.

The aim is to show to what extent an AR(2) process is a wrong discretization of an underdamped process, when it is employed for simulation purposes. We simulate multiple trajectories of the continuous linear process:

$$\begin{aligned} dx &= v dt \\ dv &= -\eta v dt - k x dt + dW \end{aligned} \tag{S1}$$

via the Euler-Maruyama scheme:

$$\begin{aligned} X_{n+1} &= X_n + V_n \tau_{sim} \\ V_{n+1} &= V_n - \eta \tau_{sim} V_n - k X_n \tau_{sim} + \sqrt{2T\eta\tau_{sim}} r_n \end{aligned} \tag{S2}$$

with  $r_n \sim \mathcal{N}(0, 1)$  I.I.D. and given initial conditions  $X_0 = 0, V_0 = 0$ . Simulations are however long enough ( $5 \cdot 10^6$  steps for each sample trajectory) that the exact value of the initial condition is irrelevant, if not too far from the steady-state mean. For the sake of simplicity, we take all parameter values equal to 1. We perform different sets of simulations (15 trajectories each) with different integration steps,  $\tau_{sim}$ , as indicated in Fig. 1 in the main text.

From each of those simulations, we firstly compute the empirical autocorrelation function:

$$\hat{C}(t = h\tau_{sim}) = \frac{1}{N-h} \sum_{n=0}^{N-h} x_n x_{n+h} \tag{S3}$$

where  $N$  is the total number of steps. Fig. 1a is an aggregated plot of all the autocorrelation functions obtained from the simulations, with various  $\tau_{sim}$ . The true autocorrelation function,  $C(t)$ , can be easily computed in the linear case, and its analytical expression is reported in Eq. 2 in the main text. At small times, the function can be expanded into a Taylor series:

$$C(t) = C(0) + \dot{C}(0)t + \frac{1}{2}\ddot{C}(0)t^2 + \frac{1}{6}\dddot{C}(0)t^3 + o(t^3). \tag{S4}$$

Since  $\dot{C}(0) = 0$ , the degree-3 polynomial Eq. (S4) is in fact described only by three coefficients. Let us rename them as  $C(t) \simeq a + bt^2 + ct^3$  ( $t \ll 1$ ). We use the empirical autocorrelation function to determine the unique set of values for these three coefficients that satisfies  $\hat{C}(0) = C(0)$ ,  $\hat{C}(\tau) = C(\tau)$  and  $\hat{C}(2\tau) = C(2\tau)$ , for some small observation interval  $\tau$ . Recalling that  $\ddot{C}(0) = -T$  and  $\dddot{C}(0) = \eta T$ , the damping coefficient is now extracted from the ratio of the third and first nonzero polynomial coefficients ( $\eta = -3c/b$ ).

We observe that when  $\tau = \tau_{sim}$ , the estimate of  $\eta$  is rescaled of a factor  $3/2$ , independently of the value of  $\tau_{sim}$ . The same problem is found if one adopts the Euler-Maruyama scheme to derive approximate inference equations and applies them to true trajectories, generated by the continuous process [7, 8]. We remark that here, on the contrary, we apply inference equations (which would be unbiased for the exact process, in the  $\tau \rightarrow 0$  limit) to sample trajectories of the discrete model in Eq. (S2). An important requirement is that the inference equations are local in time, so that they are able to detect the inaccuracies of the discrete model on short scales ( $\tau \sim \tau_{sim}$ ).

Notice that there are two different sources of error in the estimation of  $\eta$  that we perform: an approximation error, due to the use of Eq. (S4) to find the parameter estimators, and an error due to the Euler discretization of the process. In order to disentangle the former from the latter, we use exact numerical simulations of the continuous process (Gillespie algorithm) to evaluate how our estimation of  $\eta$  is affected by the small time approximation, which starts to be evident for  $\tau \sim 10^{-1}$ . In Fig. 1 in the main text we correct for this source of bias, which is numerically evaluated. This allows us to show only the effect of the discretization, which is well-described by the RG recurrence relations.

## II. RENORMALIZATION GROUP FOR ARMA(2,1) PROCESSES

An autoregressive moving-average process of order  $(p, q)$ , denoted  $\text{ARMA}(p, q)$ , is a time series generated by the update equation

$$X_n = \sum_{i=1}^p \phi_i X_{n-i} + \sum_{i=1}^q \nu_i \epsilon_{n-i} + \mu \epsilon_n + c \quad (\text{S5})$$

with  $\epsilon_n \sim \mathcal{N}(0, 1)$  I.I.D.,  $\nu_i, \mu, c \in \mathbb{R}$ . In the following, we will take  $c = 0$  (zero average ARMA process) and rename the random increment as  $r_n = \sum_{i=1}^q \nu_i \epsilon_{n-i} + \mu \epsilon_n$ .

We apply to autoregressive time-series models a Renormalization Group (RG) procedure inspired to Migdal-Kadanoff renormalization of one-dimensional spin chains. In this analogy, discretely observed states of the system play the role of spin variables sitting on lattice sites, and time steps correspond to lattice spacings. Each RG iteration consists of two operations:

1. coarse-graining by decimation, i.e. we derive the update equations for the subseries of even time states;
2. joint rescaling of the time step,  $2\tau \rightarrow \tau$ , and of the parameters of the model, according to their physical dimension.

The starting point of interest for us is the Euler discretization of the following linear process:

$$dx = vdt \quad (\text{S6})$$

$$dv = -\eta vdt - kxdt + \sigma dW, \quad (\text{S7})$$

which corresponds to the AR(2) process

$$X_{n+1} - 2X_n + X_{n-1} + \eta\tau(X_n - X_{n-1}) + k\tau^2 X_{n-1} = \sigma\tau^{3/2} \epsilon_{n+1}, \quad (\text{S8})$$

$\epsilon_n \sim \mathcal{N}(0, 1)$  I.I.D.. Let us rename  $\phi_1 = 2 - \eta\tau$ ,  $\phi_2 = -(1 - \eta\tau + k\tau^2)$ , so that Eq. (S8) is rewritten as

$$X_n = \sum_{i=1}^2 \phi_i X_{n-i} + \sigma \epsilon_n. \quad (\text{S9})$$

Coarse graining is obtained for any  $\text{AR}(2, q)$  process by taking the combination  $X_n + \phi_1 X_{n-1} - \phi_2 X_{n-2}$  (see Sec. III):

$$X_n + \phi_1 X_{n-1} - \phi_2 X_{n-2} = \sum_{i=1}^2 \phi_i X_{n-i} + \sigma \epsilon_n + \phi_1 \left( \sum_{i=1}^2 \phi_i X_{n-1-i} + \sigma \epsilon_{n-1} \right) - \phi_2 \left( \sum_{i=1}^2 \phi_i X_{n-2-i} + \sigma \epsilon_{n-2} \right), \quad (\text{S10})$$

which yields the dynamical law for the ‘even sub-lattice’ time series:

$$X_n = \sum_{i=1}^2 \tilde{\phi}_i X_{n-2i} + \tilde{r}_n, \quad (\text{S11})$$

where  $\tilde{r}_n$  is the random increment of the coarse-grained process. If we start from the AR(2) process (S9), i.e.  $q = 0$ , the new parameters are  $\tilde{\phi}_1 = (\phi_1^2 + 2\phi_2)$ ,  $\tilde{\phi}_2 = -\phi_2^2$ , and the new random increment  $\tilde{r}_n$  is defined as

$$\tilde{r}_n = \epsilon_n + \phi_1 \epsilon_{n-1} - \phi_2 \epsilon_{n-2}. \quad (\text{S12})$$

Thus,  $\mathbb{E}[\tilde{r}_n \tilde{r}_{n\pm 2}] \neq 0$ , meaning that at the first iteration we already fall into a linear ARMA(2,1) model. Luckily, the structure of ARMA(2,1) models is left unchanged by further iterations of this procedure, as shown in Sec. III.

Let us then perform a general RG iteration on the ARMA(2,1) process

$$X_n = \sum_{i=1}^2 \phi_i^l X_{n-i} + \mu^l \epsilon_n + \nu^l \epsilon_{n-1} \quad (\text{S13})$$

with running parameters  $\phi_{i \in \{1,2\}}^l, \mu^l, \nu^l$ . The aforementioned combination gives the coarse-grained stochastic difference equation

$$X_n = ((\phi_1^l)^2 + 2\phi_2^l) X_{n-2} - (\phi_2^l)^2 X_{n-4} + \tilde{r}_n^l \quad (\text{S14})$$

where

$$\tilde{r}_n^l = \mu^l \epsilon_n + (\nu^l + \phi_1 \mu^l) \epsilon_{n-1} + (\phi_1 \nu^l - \phi_2 \mu^l) \epsilon_{n-2} - \phi_2 \nu^l \epsilon_{n-3}. \quad (\text{S15})$$

Therefore the covariance of the series of random increments is specified by

$$\mathbb{E}[(\tilde{r}_n^l)^2] = [(\mu^l)^2 + (\nu^l)^2] [1 + (\phi_1^l)^2 + (\phi_2^l)^2] + 2\mu^l \nu^l \phi_1^l (1 - \phi_2^l); \quad (\text{S16})$$

$$\mathbb{E}[\tilde{r}_n^l \tilde{r}_{n\pm 2}^l] = \mu^l \nu^l \phi_1^l (1 - \phi_2^l) - \phi_2^l [(\mu^l)^2 + (\nu^l)^2]. \quad (\text{S17})$$

For a linear additive process like the one we considered above, the covariance matrix is a symmetric tridiagonal Toeplitz matrix, fully specified by these two entries. One can easily verify that  $\mathbb{E}[\tilde{r}_n^l \tilde{r}_{n\pm 2k}^l] = 0$  for  $k > 1$ .

At this point, in order to fully set the stage for the expected rescaling operation, one can exploit the fact that linear combinations of Gaussian variables are still Gaussian. Hence the random increment  $\tilde{r}_n^l$  is decomposed in the following way:

$$\tilde{r}_n^l = \tilde{\mu}^l \tilde{\epsilon}_n + \tilde{\nu}^l \tilde{\epsilon}_{n-2}, \quad (\text{S18})$$

with  $\tilde{\epsilon}_i \sim \mathcal{N}(0, 1)$  new I.I.D. variables, and  $\tilde{\mu}^l, \tilde{\nu}^l$  satisfying:

$$\mathbb{E}[(\tilde{r}_n^l)^2] = (\tilde{\mu}^l)^2 + (\tilde{\nu}^l)^2; \quad \mathbb{E}[\tilde{r}_n^l \tilde{r}_{n\pm 2}^l] = \tilde{\mu}^l \tilde{\nu}^l. \quad (\text{S19})$$

One can conveniently introduce the two running parameters  $\alpha^l = (\mu^l)^2 + (\nu^l)^2$  and  $\beta^l = \mu^l \nu^l$ , such that Eqs. (S16) and (S17), combined with Eq. (S19), become:

$$\tilde{\alpha}^l = [1 + (\phi_1^l)^2 + (\phi_2^l)^2] \alpha^l + 2\phi_1^l (1 - \phi_2^l) \beta^l; \quad (\text{S20})$$

$$\tilde{\beta}^l = \phi_1^l (1 - \phi_2^l) \beta^l - \phi_2^l \alpha^l. \quad (\text{S21})$$

Let us now consider a power series expansion for all the parameters at stake:

$$\phi_1 = \sum_{k=0}^{\infty} \psi_k \tau^k; \quad \phi_2 = \sum_{k=0}^{\infty} \theta_k \tau^k \quad (\text{S22})$$

$$\alpha = \sum_{k=0}^{\infty} \alpha_k \tau^k; \quad \beta = \sum_{k=0}^{\infty} \beta_k \tau^k. \quad (\text{S23})$$

This expansion is necessary because the parameters of the ARMA(2,1) model are dimensionless, and it would not be clear how to perform the rescaling step on them otherwise. Each coefficient in the series expansions (S22)–(S23) is a running parameter that gets rescaled according to its physical dimension (in time units). Denoting with  $w$  any of the parameters in (S22)–(S23),

$$w_k^{l+1} = 2^{-k} \tilde{w}_k^l. \quad (\text{S24})$$

Recurrence equations are then obtained applying Eq.(S24) to Eqs. (S20)–(S21) and to the coarse-grained autoregressive (AR) coefficients:

$$\tilde{\phi}_1^l = (\phi_1^l)^2 + 2\phi_2^l; \quad \tilde{\phi}_2^l = -(\phi_2^l)^2. \quad (\text{S25})$$

Equating order by order, one finds a layered set of recurrence relations that we analyze in the following sections.

### AR coefficients

Since the recurrence relations for  $\phi_1$  and  $\phi_2$  are independent of those for  $\alpha$  and  $\beta$ , let us start with the coefficients of the autoregressive (AR) part of the model. Using Eqs. (S22) and (S25) one finds

$$\tilde{\psi}_k^l = 2\theta_k^l + \sum_{i=0}^k \psi_i^l \psi_{k-i}^l; \quad \tilde{\theta}_k^l = -\sum_{i=0}^k \theta_i^l \theta_{k-i}^l. \quad (\text{S26})$$

Recalling from Eq. (S24) that  $\psi_k^{l+1} = 2^{-k} \tilde{\psi}_k^l$  and  $\theta_k^{l+1} = 2^{-k} \tilde{\theta}_k^l$ , recursive relations are readily obtained. At each order of the series expansion,  $k$ , we obtain a 2D map from which the fixed points for the considered coefficients,  $(\phi_k, \theta_k)$ , can be extracted. Notice that higher order recurrence relations are coupled to lower order ones, so one can follow a typical multiscale approach to find the fixed points or eventually solve the recurrence relations. Here we are just interested in the study of the fixed points.

*0-th order*

The recursive relations at the leading order read:

$$\begin{cases} \psi_0^{l+1} = (\psi_0^l)^2 + 2\theta_0^l \\ \theta_0^{l+1} = -(\theta_0^l)^2. \end{cases} \quad (\text{S27})$$

The first remark is that only at this order the system is nonlinear; it is evident from Eq. (S26) that at any subsequent order the map is linear.

There are 4 fixed points for the recurrence relation Eq. (S27):

- A.  $(\psi_0^*, \theta_0^*) = (0, 0)$ . It is a process with null autoregressive part, i.e. a pure moving average (MA) process. Moving average contributions (eventually null) are specified by the recurrence relations for the MA coefficients.
- B.  $(\psi_0^*, \theta_0^*) = (1, 0)$ . This fixed point corresponds to a first order process of the form  $X_n = X_{n-1} + r_n$ , i.e. an ARMA(1,  $q$ ) process; the moving average order  $q$  will be determined by the recurrence relations for  $\alpha$  and  $\beta$ .
- C.  $(\psi_0^*, \theta_0^*) = (-1, -1)$ . This is an ARMA(2,  $q$ ) process, of the form  $X_n = -X_{n-1} - X_{n-2} + r_n$ . Here again the amplitude and covariance structure of the random contribution is specified by the recursion relations for  $\alpha$  and  $\beta$ .
- D.  $(\psi_0^*, \theta_0^*) = (2, -1)$ . This model is a specific case of an ARMA(2,  $q$ ) model, known as ARIMA(1, 1,  $q$ ) model [17]. Thanks to the specific value assumed by the coefficients of the AR part, one can indeed rewrite the process as  $(1 - L)^2 X_n = r_n$ , where  $L$  is the lag operator:  $LX_n = X_{n-1}$ . So  $(1 - L)$  is the discrete differencing operator and  $\{(1 - L)X_n\} = \{\bar{V}_n\}$  is the reconstructed velocity series. We leave once again the value of  $q$  unspecified for the moment, as it is determined by the analysis of the recurrence relations for the MA coefficients.

Notice that only the fixed point A is an asymptotically stable point, whose basin of attraction is the interior of the gray triangle in Fig. S1b. The other points are unstable, at least in some directions.

We are especially interested in the class of discrete-time models represented by point D, since, at the leading order, the model can be considered as a discretized version of a second order SDE of the kind  $\ddot{x} = \xi$ , with  $\xi(t)$  a white or colored Gaussian noise. Higher order contributions can modify the coefficients  $\phi_1$  and  $\phi_2$  in front of  $X_{n-1}$  and  $X_{n-2}$ , but they won't affect the interpretation of such a process as a discretization of a second order SDE; the only difference would be in the addition of position- or velocity-dependent linear forces.

*1st order*

The recurrence relations for first-order coefficients read:

$$\begin{cases} \psi_1^{l+1} = \frac{1}{2} [2\psi_0^l \psi_1^l + 2\theta_1^l] \\ \theta_1^{l+1} = \frac{1}{2} [-2\theta_0^l \theta_1^l]. \end{cases} \quad (\text{S28})$$

The study of the fixed points reveals that their number and their nature (i.e. the kind of dynamical models they correspond to) is left unchanged:

- A.  $(\psi_0^*, \theta_0^*) = (0, 0) \implies (\psi_1^*, \theta_1^*) = (0, 0)$ . The process is still a MA process.
- B.  $(\psi_0^*, \theta_0^*) = (1, 0) \implies (\psi_1^*, \theta_1^*) = (u, 0)$  where  $u$  is a free parameter. The process is still an ARMA(1,  $q$ ) process, but it's represented by a manifold of fixed points in the space of first order coefficients.
- C.  $(\psi_0^*, \theta_0^*) = (-1, -1) \implies (\psi_1^*, \theta_1^*) = (u, 2u)$ . As for the previous fixed point, even for this unstable ARMA(2,  $q$ ) process the dimension of the fixed point manifold is increased of 1 when we move from the 0-th order to the 1st order of the series expansion.
- D.  $(\psi_0^*, \theta_0^*) = (2, -1) \implies (\psi_1^*, \theta_1^*) = (u, -u)$ . In this case the equation of motion becomes  $(1 - L)(1 - \psi_1^* L)X_n = r_n$ , still corresponding to a class of ARIMA(1, 1,  $q$ ) processes.

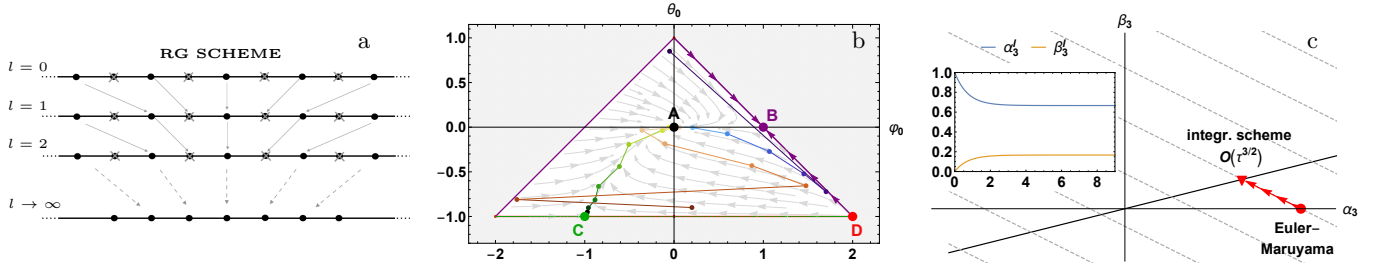


FIG. S1: (a) Sketch of the RG procedure for ARMA processes: the discrete time series is firstly decimated and then rescaled, so that the time step/lattice spacing is always kept equal to  $\tau$ . (b) Fixed points on the plane of leading order AR coefficients. For a description of the figure, see the main text. (c) RG flow on the plane of third order MA coefficients for  $s = 0$ . The black solid line is the manifold of fixed points  $\alpha_3^* = 4\beta_3^*$ . The dashed parallel lines represent different orbits associated to the solution (S56) of the linear system. A Euler-Maruyama discretization of a 2nd-order SDE corresponds to an initial condition  $(\sigma^2, 0)$  on the positive  $\alpha_3$  axis, which flows towards the ARMA(2,1) fixed point of coordinates  $(2/3, 1/6)\sigma^2$  with an  $l$ -dependent decay shown in the inset. When  $s \neq 0$  the picture above is just slightly modified, as the RG map becomes an affine one.

2nd order

Given the recurrence relations:

$$\begin{cases} \psi_2^{l+1} = \frac{1}{4} [2\psi_0^l \psi_2^l + (\psi_1^l)^2 + 2\theta_2^l] \\ \theta_2^{l+1} = -\frac{1}{4} [2\theta_0^l \theta_2^l + (\theta_1^l)^2], \end{cases} \quad (\text{S29})$$

the fixed points, at this order, are expanded as follows:

- A.  $(\psi_0^*, \theta_0^*, \psi_1^*, \theta_1^*) = (0, 0, 0, 0) \implies (\psi_2^*, \theta_2^*) = (0, 0)$ . No increase in the dimension of the manifold nor change in the nature of the process is registered.
- B.  $(\psi_0^*, \theta_0^*, \psi_1^*, \theta_1^*) = (1, 0, u, 0) \implies (\psi_2^*, \theta_2^*) = (u^2/2, 0)$ . The ARMA(1, $q$ ) nature of the model is left unchanged.
- C.  $(\psi_0^*, \theta_0^*, \psi_1^*, \theta_1^*) = (-1, -1, u, 2u) \implies (\psi_2^*, \theta_2^*) = (-u^2/2, -2u^2)$ . The values of these parameters are fixed by the values of lower order parameters, as it happened for the previous fixed point. Hence the dimension of the fixed point manifold doesn't change here.
- D.  $(\psi_0^*, \theta_0^*, \psi_1^*, \theta_1^*) = (2, -1, u, -u) \implies (\psi_2^*, \theta_2^*) = (z, -u^2/2)$ . The additional arbitrariness on  $\psi_2^*$  accommodates an  $x$ -dependent force in the second-order continuous-time SDE, from which the discrete model can be derived. The discretization picture above keeps holding, even if the ARIMA(1,1, $q$ ) structure is lost in favor of an ARMA(2, $q$ ) one, when  $\psi_2^* \neq u^2/2$ .

TABLE S1: Fixed points. The last model is, up to  $O(\tau)$ , an ARIMA(1,1,1), for any value of the free parameter  $u$ .

	Model	$\psi_0^*$	$\theta_0^*$	$\psi_1^*$	$\theta_1^*$	$\psi_2^*$	$\theta_2^*$	$\psi_3^*$	$\theta_3^*$
A.	MA( $q$ )	0	0	0	0	0	0	0	0
B.	ARMA(1, $q$ )	1	0	$u$	0	$u^2/2$	0	$u^3/6$	0
C.	ARMA(2, $q$ )	-1	-1	$u$	$2u$	$-u^2/2$	$-2u^2$	$u^3/6$	$(2u)^3/6$
D.	AR(I)MA(2, $q$ )	2	-1	$u$	$-u$	$z$	$-u^2/2$	$u(6z - u^2)/12$	$-u^3/6$

Of course the study of the fixed points can be developed to any desired order, but the discussion we made so far is already sufficient to characterize their autoregressive nature. We summarize in Table S1 the results for the coefficients of the series expansion up to the third order. The fact that the AR order of the fixed points is left unchanged at subsequent orders in the expansion can be proven by induction on Eq. (S26). Specifically, the following facts hold:

1. The autoregressive (AR) order of fixed point A is exactly zero, since  $\psi_k = \theta_k = 0 \forall k$ .
2. For fixed point B,  $\theta_k = 0 \forall k$ , ensuring it is a process of AR order equal to one. Since  $\psi_k = \frac{\psi_1^k}{k!}$ , the non-vanishing autoregressive parameter is  $\phi_1(\tau) = e^{\psi_1 \tau}$ . This fixed point corresponds to the exact discretization of a first order deterministic linear process of the kind  $\dot{x} = \psi_1 x$ , with  $\psi_1 = u$  arbitrary parameter.

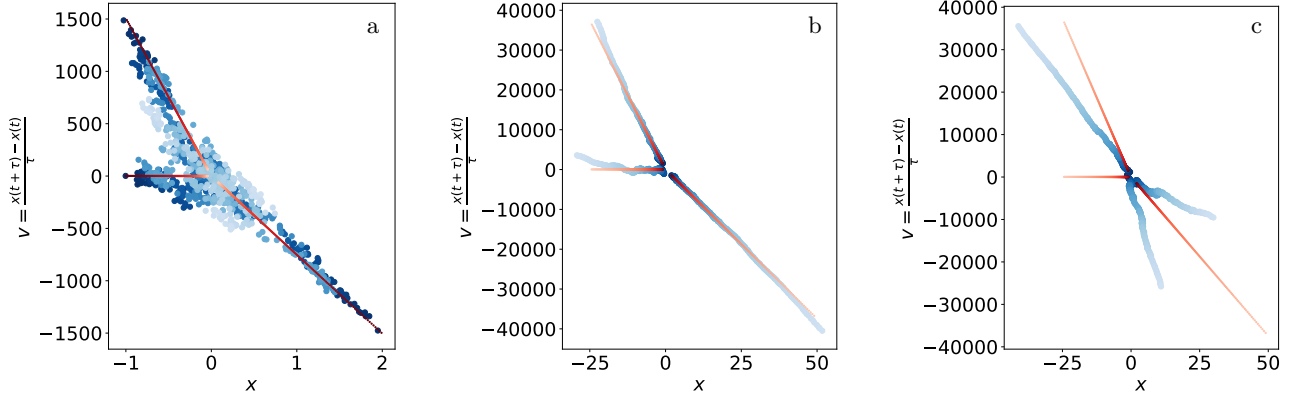


FIG. S2: Sample trajectory in the phase diagram of the fixed point process C. Red points are obtained iterating the deterministic process  $X_n = \phi_1 X_{n-1} + \phi_2 X_{n-2}$ , with  $\phi_1 = -e^{-\psi_1 \tau}$  and  $\phi_2 = -e^{-2\psi_1 \tau}$ . Blue points correspond to the stochastic fixed point process, with MA coefficients from Table S2. Color code from dark to light indicates advancing time. The deterministic model exhibits a three-branched phase diagram: at each iteration the system jumps from one branch to the next one, moving towards the origin or far from it depending on the modulus of the complex eigenvalues. (a) When  $\psi_1 > 0$  the origin is an asymptotically stable fixed point ( $\psi_1 = 2$ ,  $s = 0.5$ ,  $\tau = 0.002$ ). (b-c) The origin becomes unstable for negative  $\psi_1$ . We plot two samples with parameter values  $\psi_1 = -2$ ,  $s = 2$ ,  $\tau = 0.002$ . The presence of noise in the unstable case may give rise to very different phase diagrams from the deterministic one, if a large stochastic deviation occurs at small times (cfr Figs. 2b and 2c).

3. Fixed point C satisfies  $\psi_k = -\frac{(-\psi_1)^k}{k!}$  and  $\theta_k = -\frac{(-2\psi_1)^k}{k!}$ , implying  $\phi_1(\tau) = -e^{-\psi_1 \tau}$  and  $\phi_2(\tau) = -e^{-2\psi_1 \tau}$ . In this case no relevant continuous-time interpretation holds, as far as we know. The process has a three-branched phase diagram, and evolves in time jumping from one branch to the next one – approaching the origin or moving away from it depending on the sign of  $\psi_1$  (see Fig. S2). This structure is invariant under the RG transformation we defined, and it is precisely determined by the details of the decimation procedure. If the coarse graining procedure were implemented differently, for instance by trimming two points out of three, the same process would not be a fixed point.
4. For fixed point D we have  $\theta_k = -\frac{\psi_1^k}{k!}$ , so that  $\phi_2(\tau) = -e^{\psi_1 \tau}$ . As regards the other AR parameter, one can prove by induction that  $\psi_0 = 2$ ,  $\psi_{k \geq 1} = \frac{\psi_1^k}{k!}$  is a fixed point solution, corresponding to  $\phi_1(\tau) = 1 + e^{\psi_1 \tau}$ . The associated  $z$  parameter is equal to  $\psi_1^2/2$  in Table S1. In this case the process is an ARIMA(1,1, $q$ ) model, the deterministic part being the discretization of a linear first order process for the velocity variables:  $\ddot{x} = \psi_1 \dot{x}$ . This is not, however, the only fixed point solution; additional arbitrariness, expressed by the free parameter  $z$ , can be accommodated to take into account additional linear forces, which transform the previous equation into  $\ddot{x} = \psi_1 \dot{x} + \mathcal{K}x$ , where the  $\mathcal{K}$  parameter is a function of  $\psi_1$  and  $\psi_2$ .

### MA coefficients

Recurrence relations for the MA coefficients  $\mu$ ,  $\nu$  or, equivalently, for the parameters  $\alpha$ ,  $\beta$ , depend on those of the AR coefficients as shown above. The great advantage of working with  $\alpha$  and  $\beta$  is that, when the AR coefficients are fixed, their recurrence relations are linear:

$$\tilde{\alpha}_k^l = (1 + \psi_0^2 + \theta_0^2)\alpha_k^l + 2\beta_k^l\psi_0(1 - \theta_0) + \sum_{i=0}^{k-1} \left[ \alpha_i^l \sum_{j=0}^{k-i} (\psi_j\psi_{k-i-j} + \theta_j\theta_{k-i-j}) + 2\beta_i\psi_{k-i}(1 - \theta_0) - 2\beta_i \sum_{j=0}^{k-i-1} \psi_j\theta_{k-i-j} \right] \quad (\text{S30})$$

$$\tilde{\beta}_k^l = \beta_k^l\psi_0(1 - \theta_0) - \alpha_k^l\theta_0 - \sum_{i=0}^{k-1} \alpha_i^l\theta_{k-i} + \sum_{i=0}^{k-1} \beta_i^l \left[ \psi_{k-i}(1 - \theta_0) - \sum_{j=0}^{k-i-1} \psi_j\theta_{k-i-j} \right]. \quad (\text{S31})$$

We analyze their behaviour for each of the 4 fixed points we found for  $\phi_1$  and  $\phi_2$ .

## 0th order

At the leading order we have a homogeneous system

$$\begin{cases} \alpha_0^{l+1} = (1 + \psi_0^2 + \theta_0^2) \alpha_0^l + 2\psi_0(1 - \theta_0)\beta_0^l \\ \beta_0^{l+1} = \psi_0(1 - \theta_0)\beta_0^l - \theta_0\alpha_0^l \end{cases} \quad (\text{S32})$$

whose single fixed point is the origin  $(\alpha_0^*, \beta_0^*) = (0, 0)$ , unless the coefficients  $\theta_0$  and  $\phi_0$  take values that render the fixed point equations linearly dependent. This happens only for the fixed point A, where the condition  $(\psi_0^*, \theta_0^*) = (0, 0)$  leaves  $\alpha_0^*$  as a free parameter, while  $\beta_0^* = 0$ . As a result,  $q = 0$ , and the fixed point model is just a sequence of I.I.D. Gaussian variables.

For autoregressive models (i.e. fixed points B-D), the condition  $(\alpha_0^*, \beta_0^*) = (0, 0)$  tells us that  $\tau$ -independent noise contributions are prohibited.

## 1st order

Moving to a first order expansion (the lowest nontrivial one for the last three fixed points), recursion relations take the form of a 2D affine map:

$$\begin{cases} \alpha_1^{l+1} = \frac{1}{2} \{ (1 + \psi_0^2 + \theta_0^2) \alpha_1^l + 2(\psi_0\psi_1 + \theta_0\theta_1) \alpha_0^l + 2\psi_0(1 - \theta_0) \beta_1^l + 2[\psi_1(1 - \theta_0) - \psi_0\theta_1] \beta_0^l \} \\ \beta_1^{l+1} = \frac{1}{2} \{ \psi_0(1 - \theta_0) \beta_1^l + [\psi_1(1 - \theta_0) - \psi_0\theta_1] \beta_0^l - \theta_0\alpha_1^l - \theta_1\alpha_0^l \} \end{cases} \quad (\text{S33})$$

Fixed points:

- A. MA( $q$ ):  $(\alpha_0^*, \beta_0^*) = (s, 0) \implies (\alpha_1^*, \beta_1^*) = (0, 0)$ . Even at this order, the process results to be a degenerate MA process, with  $q = 0$ .
- B. ARMA(1, $q$ ):  $(\alpha_0^*, \beta_0^*) = (0, 0) \implies (\alpha_1^*, \beta_1^*) = (s, 0)$ , with  $s$  a free parameter. As expected, here again  $q = 0$  and the process reduces to a simple AR(1) model.
- C. ARMA(2, $q$ ):  $(\alpha_0^*, \beta_0^*) = (0, 0) \implies (\alpha_1^*, \beta_1^*) = (4s, s)$ ,  $s \in \mathbb{R}$ . We have a manifold of fixed points, represented by a line on the plane of first order covariance coefficients.
- D. AR(I)MA(2, $q$ ):  $(\alpha_0^*, \beta_0^*) = (0, 0) \implies (\alpha_1^*, \beta_1^*) = (-2s, s)$ . Even in this case, we have a line of fixed point solutions. Interestingly, the corresponding process can be interpreted as the first order discretization of a partially observed Markov process. Suppose that the measurement consists of a projection onto the  $x$  coordinate of the process described by the following set of stochastic differential equations:

$$dx = vdt + \sigma_x dW_x \quad (\text{S34})$$

$$dv = -\eta vdt - kxdx + \sigma_v dW_v \quad (\text{S35})$$

where  $W_x$  and  $W_v$  are independent Wiener processes. When  $\sigma_x \neq 0$ , the  $x$  process is discretized as an ARMA(2,1) process, even adopting an  $O(\tau^{1/2})$  Taylor-Itô expansion. This fact explains the presence of non-null coefficients  $\alpha_1, \beta_1$  at this order. On the contrary, in the case of purely inertial models, the Euler-Maruyama integrator (corresponding to  $O(\tau^{1/2})$  Taylor-Itô expansion) yields an AR(2) process. Purely inertial models can be viewed as a singular case of the class of models described by Eq. (S46), with  $\sigma_x = 0$ . If  $\sigma_x = 0$ , we should assume  $\alpha_1 = \beta_1 = 0$ , and the first non-null coefficients of the series expansion will appear at the third order. A more detailed discussion is postponed to Sec. IV.

## 2nd order

Let us write the recurrence relations for second order coefficients

$$\begin{cases} \alpha_2^{l+1} = \frac{1}{4} \{ (1 + \psi_0^2 + \theta_0^2) \alpha_2^l + 2(\psi_0\psi_1 + \theta_0\theta_1) \alpha_1^l + (2\psi_0\psi_2 + \psi_1^2 + 2\theta_0\theta_2 + \theta_1^2) \alpha_0^l + 2\psi_0(1 - \theta_0) \beta_2^l + 2[\psi_1(1 - \theta_0) - \psi_0\theta_1] \beta_1^l + 2[\psi_2(1 - \theta_0) - \psi_1\theta_1 - \psi_0\theta_2] \beta_0^l \} \\ \beta_2^{l+1} = \frac{1}{4} \{ \psi_0(1 - \theta_0) \beta_2^l + [\psi_1(1 - \theta_0) - \psi_0\theta_1] \beta_1^l + [\psi_2(1 - \theta_0) - \psi_0\theta_2] \beta_0^l - \theta_0\alpha_2^l - \theta_1\alpha_1^l - \theta_2\alpha_0^l \} \end{cases} \quad (\text{S36})$$

and analyze the fixed points:

- A. MA( $q$ ):  $(\alpha_0^*, \beta_0^*, \alpha_1^*, \beta_1^*) = (s, 0, 0, 0) \implies (\alpha_2^*, \beta_2^*) = (0, 0)$  i.e.  $q = 0$  at this order too.
- B. ARMA(1, $q$ ):  $(\alpha_0^*, \beta_0^*, \alpha_1^*, \beta_1^*) = (0, 0, s, 0) \implies (\alpha_2^*, \beta_2^*) = \psi_1(s, 0)$ . The process is still memoryless –  $q = 0$  – as  $\beta_2^* = 0$ , while  $\alpha_2^*$  is generally nonzero. Notice, however, that this coefficient is not an arbitrary parameter, but determined by the values of  $\psi_1$  and of the lower order coefficient  $\alpha_1^*$ .
- C. ARMA(2, $q$ ):  $(\alpha_0^*, \beta_0^*, \alpha_1^*, \beta_1^*) = (0, 0, 4s, s) \implies (\alpha_2^*, \beta_2^*) = -2\psi_1(4s, s)$ . As a consequence, the relation between diagonal and off-diagonal entries of the covariance matrix of the random increments is left unchanged going from first to second order:  $\alpha_2^* = 4\beta_2^*$ .
- D. AR(I)MA(2, $q$ ):  $(\alpha_0^*, \beta_0^*, \alpha_1^*, \beta_1^*) = (0, 0, -2s, s) \implies (\alpha_2^*, \beta_2^*) = \psi_1(-2s, s)$ . As in the previous points, no new free parameter is introduced at this level.

### 3rd order

We report the recurrence relations for third order coefficients by replacing directly  $\beta_0^l = 0$ :

$$\begin{cases} \alpha_3^{l+1} = \frac{1}{8} \{ (1 + \psi_0^2 + \theta_0^2) \alpha_3^l + 2(\psi_0 \psi_1 + \theta_0 \theta_1) \alpha_2^l + (2\psi_0 \psi_2 + \psi_1^2 + 2\theta_0 \theta_2 + \theta_1^2) \alpha_1^l + 2(\psi_0 \psi_3 + \psi_1 \psi_2 + \theta_3 \theta_0 \\ \quad + \theta_1 \theta_2) \alpha_0^l + 2\psi_0(1 - \theta_0) \beta_3^l + 2[\psi_1(1 - \theta_0) - \psi_0 \theta_1] \beta_2^l + 2[\psi_2(1 - \theta_0) - \psi_1 \theta_1 - \psi_0 \theta_2] \beta_1^l \\ \beta_3^{l+1} = \frac{1}{8} \{ \psi_0(1 - \theta_0) \beta_3^l + [\psi_1(1 - \theta_0) - \psi_0 \theta_1] \beta_2^l + [\psi_2(1 - \theta_0) - \psi_0 \theta_2] \beta_1^l - \theta_0 \alpha_3^l - \theta_1 \alpha_2^l - \theta_2 \alpha_1^l - \theta_3 \alpha_0^l \} . \end{cases} \quad (\text{S37})$$

Fixed points:

- A. MA( $q$ ):  $(\alpha_0^*, \beta_0^*, \alpha_1^*, \beta_1^*, \alpha_2^*, \beta_2^*) = (s, 0, 0, 0, 0, 0) \implies (\alpha_3^*, \beta_3^*) = (0, 0)$ . We conclude that the unique stable fixed point is just a sequence of random I.I.D. Gaussian variables.
- B. ARMA(1, $q$ ):  $(\alpha_0^*, \beta_0^*, \alpha_1^*, \beta_1^*, \alpha_2^*, \beta_2^*) = (0, 0, s, 0, \psi_1 s, 0) \implies (\alpha_3^*, \beta_3^*) = (\frac{2}{3} \psi_1^2 s, 0)$ . Even at this order, the process is an AR(1) model, without memory nor color. It is proven by induction that this holds true at any subsequent order.
- C. ARMA(2, $q$ ):  $(\alpha_0^*, \beta_0^*, \alpha_1^*, \beta_1^*, \alpha_2^*, \beta_2^*) = (0, 0, 4s, s, -8\psi_1 s, -2\psi_1 s) \implies (\alpha_3^*, \beta_3^*) = (\frac{32}{3} \psi_1^2 s, \frac{13}{6} \psi_1^2 s)$ . The relation between diagonal and off-diagonal entries of the covariance matrix of the random increments is no more the same we had at lower orders, but no new free parameter is introduced.
- D. AR(I)MA(2, $q$ ):  $(\alpha_0^*, \beta_0^*, \alpha_1^*, \beta_1^*, \alpha_2^*, \beta_2^*) = (0, 0, -2s, s, -2\psi_1 s, \psi_1 s) \implies (\alpha_3^*, \beta_3^*) = (4b - (2\psi_2 + 3\psi_1^2)s, b)$ . For this nontrivial fixed point, the third order recurrence relations are linearly dependent, and admit infinitely many solutions parametrized by, e.g.,  $\beta_3^* = b$ . The additional arbitrariness we find at this order comes from the fact that this fixed point model corresponds to the discretized version of Eqs. (S34)–(S35). The presence of a dynamical noise source acting on the unobserved degree of freedom  $v$  results into an  $O(\tau^3)$  contribution for the covariance matrix entries which is independent of the previous  $O(\tau)$  contribution. A broader discussion about this fourth fixed point of physical interest can be found in Sec. IV.

Table S2 summarizes the findings related to the MA coefficients of the 4 fixed points. Notice that, in addition to the reported 4 fixed points, there is also the diverging fixed point, having  $\psi_k^* = \theta_k^* = \infty$ ,  $\alpha_k^* = \beta_k^* = \infty \forall k$ .

TABLE S2: Fixed points – MA coefficients. Fixed point models are reported in the same order as in Table S1, specifying here the moving average order associated to each. We denote  $u = \psi_1^*$ ,  $z = \psi_2^*$ .

	Model	$\alpha_0^*$	$\beta_0^*$	$\alpha_1^*$	$\beta_1^*$	$\alpha_2^*$	$\beta_2^*$	$\alpha_3^*$	$\beta_3^*$
A.	MA(0)	$s$	0	0	0	0	0	0	0
B.	AR(1)	0	0	$s$	0	$us$	0	$2u^2 s/3$	0
C.	ARMA(2,1)	0	0	$4s$	$s$	$-8us$	$-2us$	$32u^2 s/3$	$13u^2 s/6$
D.	AR(I)MA(2,1)	0	0	$-2s$	$s$	$-2us$	$us$	$4b - (2z + 3u^2)s$	$b$

Induction can be applied also to the recursion relations of the MA coefficients to show that the nature of the fixed points is left unchanged if one takes higher order expansions. In particular, one can prove that

1. Fixed point A is a pure random sequence of IID Gaussian variables. The only non-null parameter is  $\alpha_0$ , while  $\beta_k = 0$  and  $\alpha_j = 0$  for any  $k \geq 0$  and  $j \geq 1$ .
2. Fixed point B is at any order a simple autoregressive process of order one, AR(1), since  $\beta_k = 0 \forall k$ . The variance of the random increment is reconstructed as the series expansion with coefficients  $\alpha_0 = 0$ ,  $\alpha_k = \alpha_1 \frac{(2\psi_1)^{k-1}}{k!}$  for  $k \geq 1$ . Hence,  $\alpha(\tau) = \frac{\alpha_1}{2\psi_1} (e^{2\psi_1\tau} - 1)$ .

### III. DECIMATION OF GENERAL ARMA( $p, q$ ) MODELS

We show in this section that, given a general ARMA( $p, q$ ) model:

$$X_n = \sum_{i=1}^p \phi_i X_{n-i} + \sum_{j=1}^q \mu_j \epsilon_{n-j} + \mu_0 \epsilon_n, \quad (\text{S38})$$

there must exist a specific relation between  $p$  and  $q$  if the property of invariance under coarse-graining is required.

Let us adopt the strategy of decimation for coarse-graining: we want to trim a point out of two in the time sequence generated by Eq. (S38), as sketched in Fig. S1a. In order to obtain effective ARMA( $p, q$ ) equations on a doubled time scale, one should simply use the linear combination  $X_n + \sum_{i=1}^p (-1)^{i+1} \phi_i X_{n-i}$ . The resulting discrete-time model reads:

$$\begin{aligned} X_n = & \sum_{i=1}^p [1 + (-1)^i] \phi_i X_{n-i} + \sum_{i=1}^p (-1)^{i+1} \phi_i \sum_{k=1}^p \phi_k X_{n-k-i} + \mu_0 \epsilon_n \\ & + \sum_{j=1}^q \mu_j \epsilon_{n-j} + \sum_{i=1}^p (-1)^{i+1} \phi_i \left[ \mu_0 \epsilon_{n-i} + \sum_{k=1}^q \mu_k \epsilon_{n-i-k} \right]. \end{aligned} \quad (\text{S39})$$

The second sum in Eq. (S39) can be cast into a recursive structure:

$$\sum_{i=1}^p (-1)^{i+1} \phi_i \sum_{k=1}^p \phi_k X_{n-k-i} = \phi_1^2 X_{n-2} + 2\phi_1 \sum_{k=1}^{\lfloor \frac{p-1}{2} \rfloor} \phi_{2k+1} X_{n-2-2k} + \sum_{i=2}^p (-1)^{i+1} \phi_i \sum_{k=2}^p \phi_k X_{n-k-i}, \quad (\text{S40})$$

as the last term in Eq. (S40) can be rewritten as  $-\sum_{i=1}^{p-1} (-1)^{i+1} \phi_{i+1} \sum_{k=1}^{p-1} \phi_{k+1} X_{n-2-k-i}$  and the same decomposition used to derive Eq. (S40) can be repeatedly applied. As a result:

$$\sum_{i=1}^p (-1)^{i+1} \phi_i \sum_{k=1}^p \phi_k X_{n-k-i} = \sum_{i=1}^p (-1)^{i+1} \left( \phi_i^2 X_{n-2i} + 2 \sum_{k=i}^{\lfloor \frac{p-1}{2} \rfloor} \phi_i \phi_{2k+1} X_{n-2k-2} \right). \quad (\text{S41})$$

The final expression obtained in Eq. (S41) shows that, after the decimation, one maintains an autoregressive part of order  $p$ . On the contrary, the first sum on the r.h.s. of Eq. (S39) is equal to  $2 \sum_{i=1}^{\lfloor p/2 \rfloor} \phi_{2i} X_{n-2i}$  and only contributes up to an AR order  $\lfloor p/2 \rfloor$ .

What remains to determine is whether there is an ‘invariant MA order’  $q$  associated to  $p$ . Let us rewrite the full decimated equation

$$X_n = \sum_{i=1}^{\lfloor p/2 \rfloor} 2\phi_{2i} X_{n-2i} + \sum_{i=1}^p (-1)^{i+1} \left( \phi_i^2 X_{n-2i} + 2 \sum_{k=i}^{\lfloor \frac{p-1}{2} \rfloor} \phi_i \phi_{2k+1} X_{n-2k-2} \right) + r_n \quad (\text{S42})$$

and focus on the random term:

$$r_n = \mu_0 \epsilon_n + \sum_{j=1}^q \mu_j \epsilon_{n-j} + \sum_{i=1}^p (-1)^{i+1} \phi_i \left( \mu_0 \epsilon_{n-i} + \sum_{j=1}^q \mu_j \epsilon_{n-j-i} \right). \quad (\text{S43})$$

Since linear combinations of Gaussian variables are still Gaussian, one can redefine properly the  $\epsilon_m$ 's and rearrange the coefficients in front of them to rewrite  $r_n = \sum_{i=0}^{q'} \tilde{\mu}_i \epsilon_{n-2i}$ , where

$$q' = \left\lfloor \frac{p+q}{2} \right\rfloor. \quad (\text{S44})$$

Hence one can deduce that there are only 2 invariant scenarios for ARMA( $p, q$ ) processes:  $q = p$  or  $q = p - 1$ . When translated into the language of integration schemes for continuous-time processes, this fact tells us that the marginalization of each hidden degree of freedom does not bring only memory, increasing by one the order of the autoregressive part, but also color, increasing by one the order of the moving average part of the model. This fact is well known [19]. In a similar form, the same remark is already in [18].

Once the general invariant structure under decimation of ARMA( $p, q$ ) time series is found, the RG machinery can be deployed and a careful study of the fixed points can be carried out.

#### IV. THE FOURTH FIXED POINT

This section is devoted to a more detailed discussion of the fourth fixed point, which, due to its physical meaning, we think deserves a special focus.

We already highlighted that at leading order AR coefficients reproduce a second time derivative through the double differencing operator  $\Delta^2 = (1 - L)^2$ . This fact gives to the model an ‘integrated process’ nature, namely an ARIMA(1,1,1) structure [17]. Since the relation

$$\lim_{\tau \rightarrow 0} \frac{\phi_1 - \psi_0^*}{\tau} = - \lim_{\tau \rightarrow 0} \frac{\phi_2 - \theta_0^*}{\tau} \quad (\text{S45})$$

also holds, this integrated process structure is kept up to  $O(\tau)$ . Deviations from it occur at higher order and are due to the presence of linearly  $x$ -dependent forces. The fixed point model is indeed the consistent discretization of a general class of continuous-time processes described by Eqs. (S34)–(S35), when only the  $x$  variable can be directly observed.

Adopting the generalized Langevin equation formalism to those equations, one finds:

$$dx(t) = v_0 e^{-\eta t} dt + \left[ \int_0^t e^{-\eta(t-s)} f(x(s)) ds \right] dt + \int_0^t e^{-\eta(t-s)} \sigma_v dW_v(s) + \sigma_x dW_x(t). \quad (\text{S46})$$

The initial condition on the unobserved variable  $v_0$  is eliminated through a suitable combination of two subsequent increments on the intervals  $[0, \tau]$  and  $[\tau, 2\tau]$ :

$$\begin{aligned} x(2\tau) - (1 + e^{-\eta\tau})x(\tau) + e^{-\eta\tau}x(0) &= \int_0^{2\tau} f(x(s))\psi(s-\tau)ds + \sigma_v \int_0^{2\tau} \psi(s-\tau)dW_v(s) \\ &\quad + \sigma_x \int_\tau^{2\tau} dW_x(s) - e^{-\eta\tau}\sigma_x \int_0^\tau dW_x(s) \end{aligned} \quad (\text{S47})$$

with

$$\psi(s) = \begin{cases} \psi_+(s) = \frac{1 - e^{\eta(s-\tau)}}{\eta} & \text{for } 0 \leq s < \tau \\ \psi_-(s) = \frac{e^{\eta s} - e^{-\eta\tau}}{\eta} & \text{for } -\tau < s < 0. \end{cases} \quad (\text{S48})$$

Let us start the discussion from a simplified example:  $f(x) = 0$ . In this case the exact AR coefficients are already given:  $\phi_1 = 1 + e^{-\eta\tau}$ ,  $\phi_2 = e^{-\eta\tau}$ . Also, the covariance of the random increments can be easily computed. If we shift Eq. (S47) of  $n$  steps, by identifying  $\{x(2\tau), x(\tau), x(0)\}$  with  $\{X_n, X_{n-1}, X_{n-2}\}$ , the  $n$ -th step random increment of the ARMA process,  $r_n \equiv \mu\epsilon_n + \nu\epsilon_{n-1}$ , reads:

$$r_n = \sigma_v \int_{t_n-2\tau}^{t_n} \psi(s-\tau)dW_v(s) + \sigma_x [W_x(t_n) - W_x(t_n-\tau)] - e^{-\eta\tau}\sigma_x [W_x(t_n-\tau) - W_x(t_n-2\tau)]. \quad (\text{S49})$$

Hence

$$\mathbb{E}[r_n^2] = \alpha = \sigma_x^2 \tau (1 + e^{-2\eta\tau}) + \frac{\sigma_v^2}{\eta^2} \left[ \tau (1 + e^{-2\eta\tau}) - \frac{1}{\eta} (1 - e^{-2\eta\tau}) \right] \simeq 2\sigma_x^2 \tau (1 - \eta\tau + \eta^2 \tau^2) + \sigma_v^2 \frac{2}{3} \tau^3; \quad (\text{S50})$$

$$\mathbb{E}[r_n r_{n\pm 1}] = \beta = -e^{-\eta\tau} \sigma_x^2 \tau - \frac{\sigma_v^2}{\eta^3} \left[ \eta\tau e^{-\eta\tau} \frac{1}{2} (1 + e^{-2\eta\tau}) \right] \simeq -\sigma_x^2 \tau (1 - \eta\tau - \frac{1}{2} \eta^2 \tau^2) + \sigma_v^2 \frac{1}{6} \tau^3. \quad (\text{S51})$$

By identifying the  $\alpha_k$  and  $\beta_k$  coefficients from Eqs. (S50)–(S51), one can check that they match the results reported in Tables S1–S2, where  $u = -\eta$ ,  $z = u^2/2 = \eta^2/2$ ,  $s = \sigma_x^2$ ,  $b = \frac{1}{6} \sigma_v^2 - \frac{\eta^2}{2} \sigma_x^2$ .

In the general  $f(x) \neq 0$  case, the presence of the force modifies both AR and MA coefficients (unless  $f$  is a constant). In order to evaluate how they are affected, one can perform a Taylor-Itô expansion of the integrand up to the desired order and estimate the coefficients of the discrete-time model. It is important to remember that, since  $x(s)$  is a stochastic process, the definition of the random increment  $r_n$  does not correspond to Eq. (S49) any more; if we truncate the expansion of  $r_n$  at the order  $O(\tau^{3/2})$ , it reads:

$$r_n \simeq \sigma_v \int_{t_n-2\tau}^{t_n} \psi(s-\tau) dW_v(s) + \sigma_x [W_x(t_n) - W_x(t_n-\tau)] - e^{-\eta\tau} \sigma_x [W_x(t_n-\tau) - W_x(t_n-2\tau)] + \sigma_x f'(x(t_{n-2})) \int_{t_n-2\tau}^{t_n} \psi(s-\tau) [W(s) - W(0)] ds. \quad (\text{S52})$$

In the linear case under study,  $f'(x(t_{n-2}))$  is equal to minus the elastic constant. Let us denote the elastic constant with  $\mathcal{K}$ ; the relation with the coefficients in Table S2 is:  $-\mathcal{K} = z - u^2/2$ .

We can now compute the covariance of the random increments up to  $O(\tau^3)$  and check that the fixed-point relations are satisfied:

$$\mathbb{E}[r_n^2] \simeq 2\sigma_x^2 \tau (1 - \eta\tau + \eta^2 \tau^2) + \sigma_v^2 \frac{2}{3} \tau^3 + \frac{4}{3} \mathcal{K} \sigma_x^2 \tau^3; \quad (\text{S53})$$

$$\mathbb{E}[r_n r_{n\pm 1}] \simeq -\sigma_x^2 \tau (1 - \eta\tau - \frac{1}{2} \eta^2 \tau^2) + \sigma_v^2 \frac{1}{6} \tau^3 - \frac{1}{6} \mathcal{K} \sigma_x^2 \tau^3. \quad (\text{S54})$$

This explicitly shows that the fourth fixed point is a consistent discretization of any stochastic process of the form of Eqs. (S34)–(S35), when only the  $x$  variable is measurable.

A special role in this class is played by purely inertial models. They are defined by the condition  $\sigma_x^2 = 0$ . This condition brings a significant simplification in the discretization, since there are no  $O(\tau^{1/2})$  stochastic contributions to the observed process. As a consequence, up to third order MA coefficients are not affected by the mixing of random and conservative forces; results can be read from Table S2 setting  $s = 0$ . Because of the absence of  $O(\tau^{1/2})$  stochastic contributions, applying a Euler-Maruyama discretization to purely inertial models gives rise to an AR(2) model. On the contrary, when  $\sigma_x \neq 0$  adopting a Euler-Maruyama scheme yields an (inconsistent) ARMA(2,1) model.

Since purely inertial models can be of interest in many contexts, let us focus on them. Specifically, let us consider the recurrence relations for the MA coefficients. The condition  $\sigma_x = 0$  implies  $s = 0$ , hence null MA coefficients up to the third order. Third order recurrence relations are in this case:

$$\begin{cases} \alpha_3^{l+1} = \frac{1}{8} [6\alpha_3^l + 8\beta_3^l] \\ \beta_3^{l+1} = \frac{1}{8} [\alpha_3^l + 4\beta_3^l] \end{cases} \quad (\text{S55})$$

Orbits are lines in the  $(\alpha_3, \beta_3)$  plane:  $\alpha_3 + 2\beta_3 = c$ , being  $c$  a constant fixed by the initial condition  $(\alpha_3^0, \beta_3^0)$ . The intersection with the line of fixed points,  $\alpha_3^* = 4\beta_3^*$ , identifies in our space of parameters the model which is reached by repeatedly coarse-graining the starting discrete-time model. A schematics is in Fig.S1c. Thanks to linearity, one can also compute how the asymptotic point is approached. The solution of Eq. (S55) is

$$\begin{cases} \alpha_3^l = 4^{-l} \frac{1}{3} [\alpha_3^0 - \beta_3^0] + \frac{2}{3} [\alpha_3^0 + 2\beta_3^0] \\ \beta_3^l = 4^{-l} [\frac{2}{3} \beta_3^0 - \frac{1}{6} \alpha_3^0] + \frac{1}{6} [\alpha_3^0 + 2\beta_3^0] \end{cases} \quad (\text{S56})$$

Choosing as initial conditions  $(\alpha_3^0, \beta_3^0) = (\sigma_v^2, 0)$  means selecting the AR(2) model produced by the Euler discretization of the inertial linear process in Eqs. (S34)–(S35), with  $\sigma_x = 0$ . Under subsequent iterations of the RG procedure, the covariance matrix of random increments,  $C_{nm} = \mathbb{E}[r_n r_m]$ , is modified as follows:

$$C^0 = \sigma_v^2 \begin{pmatrix} 1 & 0 & \dots & 0 \\ 0 & 1 & & \vdots \\ \vdots & & \ddots & 0 \\ 0 & \dots & 0 & 1 \end{pmatrix} \longrightarrow C^1 = \sigma_v^2 \begin{pmatrix} 3/4 & 1/8 & \dots & 0 \\ 1/8 & 3/4 & & \vdots \\ \vdots & & \ddots & 1/8 \\ 0 & \dots & 1/8 & 3/4 \end{pmatrix} \longrightarrow \dots \longrightarrow C^\infty = \sigma_v^2 \begin{pmatrix} 2/3 & 1/6 & \dots & 0 \\ 1/6 & 2/3 & & \vdots \\ \vdots & & \ddots & 1/6 \\ 0 & \dots & 1/6 & 2/3 \end{pmatrix}. \quad (\text{S57})$$

Asymptotically, it converges to the covariance matrix of a consistent  $O(\tau^{3/2})$  integration scheme. This fact justifies that, despite the order of strong convergence of the Euler scheme is  $1/2$  and it yields inconsistencies when adopted for inferring second-order SDEs, observing the simulated process at a scale much larger than the simulation step makes it acquire an effective higher order of convergence. In other words, infinitely many Euler integration steps within a given time interval are equivalent to a single integration step on that interval performed using an integration scheme which is strongly convergent at least as  $\tau^{3/2}$ . There is then an ‘asymptotic upgrade’ of the order of convergence of the scheme, at least in the linear case. We don’t know to what extent this is extendible to the nonlinear case, since stability issues of the scheme may be relevant. It is however clear that nonlinear discrete white noise models resulting from Euler discretizations are still inappropriate. However, consistent numerical integrators are available, like [12], which has been used in [7] to develop a Bayesian inference scheme for underdamped Langevin models.

## V. EFFECTIVE AR(2) MODELS FOR GENERALIZED LANGEVIN EQUATIONS AT EQUILIBRIUM

The argument we presented so far is not based on any stationarity nor equilibrium assumption for the continuous process we observe. It only relies on the requirement that the discretized model must have an invariant structure under coarse graining. Such a requirement ensures that a transition over a time interval  $2\tau$  can be equivalently described, up to a given order of approximation, either by a discretization on a single time step of amplitude  $2\tau$  or by the composition of two  $\tau$ -steps – using the same scheme.

We saw that when this request is not satisfied, the discretization is inadequate, producing biased estimators when applied to inference problems. Given an underdamped Langevin equation like

$$dx = vdt; \quad dv = [-\eta vdt + f(x)]dt + \sqrt{2T\eta}dW, \quad (\text{S58})$$

the bias comes in the form of a  $\tau$ -independent rescaling factor equal to  $2/3$  for the linear damping coefficient  $\eta$ , whereas the remaining parameters are unbiasedly estimated. How universal is this behaviour? We conjecture that the inconsistency of the inference scheme is absorbed by such a simple rescaling for all the inertial equilibrium processes described by Eq. (S58) (i.e for any conservative  $f(x)$ , including multidimensional processes). In this section we try to provide an argument for this fact, working out the reference problem of an integrated Ornstein-Uhlenbeck (OU) process.

The integrated OU process is the simplest example of 2nd-order SDE for which the Euler-related inconsistency appears. Suppose we can only observe (with infinite accuracy) the inertial degree of freedom of a process described by the SDE (S58) with  $f(x) = 0$ . Let us recall the notation for the time series of empirical observations  $\{X_n\}_{n \in \mathbb{N}}$ , and for that of reconstructed velocities  $\{\bar{V}_n\}_{n \in \mathbb{N}}$ , where  $\bar{V}_n = (X_{n+1} - X_n)/\tau$ . Let us also introduce the series of *real* velocities  $\{V_n\}_{n \in \mathbb{N}}$ , corresponding to the one we would obtain if we were able to measure directly the velocity degree of freedom. Because the evolution of this variable is described by an independent 1st-order SDE in the OU process, the time series  $\{V_n\}_{n \in \mathbb{N}}$  is described by an AR(1) process. On the contrary, the evolution of the  $x$  variables is non Markovian and expressed, at the continuous level, via a generalized Langevin equation. Consequently, the time series  $\{\bar{V}_n\}_{n \in \mathbb{N}}$  inherits a nonzero MA order – ARMA(1,1). Nonetheless, we may ask whether it is possible to describe it with an *effective* AR(1) process, which would correspond to an effective AR(2) process for the  $\{X_n\}_{n \in \mathbb{N}}$  series.

Let us consider an AR(1) model of the following form for the series of reconstructed velocities:

$$(1 - L)\bar{V}_n + \alpha L\bar{V}_n = \sigma\epsilon_n, \quad (\text{S59})$$

where  $L$  is the aforementioned lag operator,  $\epsilon_n \sim \mathcal{N}(0, 1)$  I.I.D. and  $\alpha, \sigma$  are parameters to fix. The goal is to find an effective memoryless discrete model for  $\{\bar{V}_n\}_{n \in \mathbb{N}}$  that reproduces correctly the sufficient statistics used by Bayesian and non-Bayesian parametric inference approaches. The common characteristic of these approaches is being derived from a small  $\tau$  Taylor-Itô expansion; hence they just exploit short time information to learn the dynamic laws of the system. In the case of the integrated Ornstein-Uhlenbeck process, a sufficient statistics corresponds to the set  $\mathcal{S}_1 = \{\mathbb{E}[\bar{V}_n^2], \mathbb{E}[\bar{V}_n\bar{V}_{n+1}]\}$  of reconstructed velocity self-correlations at equal time and at a distance of one time step, or, equivalently, to the set  $\mathcal{S}_2 = \{\mathbb{E}[\bar{X}_n^2], \mathbb{E}[\bar{X}_n\bar{X}_{n+1}], \mathbb{E}[\bar{X}_n\bar{X}_{n+2}]\}$ .

We impose on these observables the two following physical conditions:

- i.  $\bar{V}_n$  follows a Maxwell Boltzmann distribution with temperature  $T$ . Since the only parameter of the distribution is the variance, this condition corresponds to equipartition ( $k_B = 1$ ):

$$\mathbb{E}[\bar{V}_n^2] = T. \quad (\text{S60})$$

- ii. The covariance of the random increment of Eq. (S59) matches the diagonal entries of the covariance of the consistent scheme of order 3/2:

$$\mathbb{E}[r_n^2] = \sigma^2 \mathbb{E}[\epsilon_n^2] = \frac{2}{3} 2T\eta\tau. \quad (\text{S61})$$

The self-correlation function  $\mathbb{E}[\bar{V}_n \bar{V}_{n+k}]$  of an AR(1) process of the form of Eq. (S59) is explicitly known:

$$\mathbb{E}[\bar{V}_n \bar{V}_{n+k}] = \frac{(1-\alpha)^{|k|} \sigma^2}{1 - (1-\alpha)^2}. \quad (\text{S62})$$

Taking its value at  $k = 0$  and imposing the condition (S60) gives the discrete counterpart of Einstein's relation:

$$\sigma^2 = T [1 - (1-\alpha)^2]. \quad (\text{S63})$$

Expanding Eq. (S63) to the lowest order in  $\tau$ , it acquires the common form  $\sigma^2 = 2T\alpha$  and yields the expected result  $\alpha = (2/3)\eta\tau$ .

In conclusion, it is possible to describe the sequence of measurements of an integrated OU process as an effective AR(2) series with a rescaled damping coefficient  $\eta' = (2/3)\eta$ . Of course, this effective discretization can only be used at the scale of  $\tau$ : it gives, by construction, consistent estimators when applied to inference problems, but cannot be iterated in simulations to reproduce the process on longer scales. Because of the convergence of Euler-Maruyama integration algorithm, the simulated process would be the underdamped Langevin process with a damping coefficient equal to  $\eta'$ .

Although the derivation is based on the linear and integrated nature of the process, which allows us to work with the reconstructed velocity series  $\{\bar{V}_n\}_{n \in \mathbb{N}}$ , we conjecture that the same results should hold for all equilibrium inertial processes described by Eq. (S58) or its multidimensional generalization (with  $f(x)$  conservative forces). In addition to the physical interpretation of the imposed conditions, the conjecture is supported by numerical results. Applying, for instance, Euler-based inference schemes to simulated time series with  $f(x) = -kx - \lambda x^3$ , one obtains consistent parameter estimators except for the damping coefficient  $\eta$ , which is just rescaled of a factor 2/3.

We hope that this consideration can help simplifying the dynamical inference procedure in those experimental contexts where the observed phenomena are modelled via underdamped equilibrium processes, and inertial degrees of freedom are the only ones to be directly accessible.